Ion-excited $K\alpha$ x-ray satellite spectra of Si, S, Cl, and Ar in the gas phase

J. A. Demarest* and R. L. Watson
Cyclotron Institute and Department of Chemistry, Texas A&M University, College Station, Texas 77843
(Received 17 October 1977)

The $K\alpha$ satellite spectra of Si in the gases SiH_4 and SiF_4, of S in the gases H_2S, SO_2, and SF_6, of Cl in the gases HCl and Cl_2 and in the liquid CCl_4, and of gaseous Ar produced by bombardment with oxygen ions were examined in detail and compared with the spectra of solid compounds obtained in a previous study. It was found that the apparent average state of L-shell ionization at the time of $K\alpha$ x-ray emission does not depend upon the physical state, but upon the availability of electrons from nearest-neighbor atoms. The $K\alpha$ satellite energies in conjunction with Hartree-Fock calculations provide a measure of the average numbers of missing M-shell electrons, and this information further supports the conclusion that interatomic electron transfer dominates the fast rearrangement occurring prior to $K\alpha$ x-ray emission in atoms having highly depleted M shells. Various $K\alpha$ satellite peak-broadening mechanisms were considered and it was found that broadening due to the distribution of M-shell vacancies accounts for a significant portion of the total peak width.

I. INTRODUCTION

Investigations of the effects of chemical environment on x-ray spectra have, over the years, provided much interesting and useful information regarding the chemical states of atoms. Although most of the studies conducted on this subject have been concerned with precise measurements of $K\alpha$ and $K\beta$ line shifts and their relationship to the character of the bonding involved, chemical effects on the satellite lines $K\alpha'$, $K\alpha_3$, and $K\alpha_4$ have also been examined in some detail.[1,2] Recently, much attention has been directed toward the study of environmental effects on the intense $K\alpha$ satellite structure produced by heavy-ion bombardment.[3-11]

A particularly interesting aspect of the work on heavy-ion excited $K\alpha$ satellite spectra has been the uncovering of a new kind of chemical effect which causes variations in the relative intensity distributions from one compound of a particular element to another. An extensive set of measurements, performed on a number of solid compounds of Al, Si, S, and Cl, has revealed that the apparent degree of L-shell ionization present at the time of $K\alpha$ x-ray emission (as reflected by the relative intensities of the satellite lines) (a) increases as the *localized* valence electron density of the target atom increases and (b) decreases as the average *total* valence electron density of the compound increases.[6,11] Other measurements performed on several gaseous compounds of Si[8,10] and S[10] have shown that the gases SiH_4 and H_2S display much higher average L-shell ionization states than do solid Si and S_8, while the average L-shell ionization states, for the heavier gases SiF_4 and SF_6, closely resemble those of solid Si and S_8, respectively.

These effects are thought to be attributable to the influence of chemical bonding on the rates of $K \rightarrow M$ and $L \rightarrow M$ vacancy transfer processes. The reasoning which leads to this conclusion is based upon the fact that in the particular cases studied, L-vacancy transfer must involve the valence levels (M shell). Hence, it is to be expected that the rates of electron transitions to the L shell will depend quite sensitively on the valence electron density, which in turn is influenced by chemical bonding. The rationalization of the experimental observations set forth above, however, requires the additional hypothesis that electron transfer from the valence levels of *neighboring* atoms effectively competes with $K\alpha$ x-ray emission, which in these highly ionized atoms occurs on a time scale of the order of 10^{-14} sec.

The results of the studies conducted thus far provide an intriguing preview of the wealth of information concerning relaxation processes for highly ionized atoms obtainable from measurements of ion-excited x-ray satellite spectra. Such work is further motivated by the need to correct for rearrangement effects in applying x-ray emission measurements to the investigation of heavy-ion collisions. Because of the complex nature of the problem, a great deal more information on a wide variety of chemical systems will be required before a detailed understanding of the factors affecting electron rearrangement in multiply ionized atoms can be achieved. Of special importance in this regard are studies which concentrate on simple systems involving isolated single molecules.

The present work was carried out for the purpose of further delineating the role of interatomic electron transfer in the fast rearrangement that follows multiple electron ejection in heavy-ion col-

lisions. The $K\alpha$ satellite spectra of Si in the gases SiH_4 and SiF_4, of S in the gases H_2S, SO_2, and SF_6, of Cl in the gases HCl, Cl_2, and in the liquid CCl_4, and of gaseous Ar have been measured under carefully controlled conditions using 32-MeV oxygen ions so as to enable detailed comparisons with the spectra obtained previously for solid compounds. In addition, the energies and intensities of $K\alpha$ satellites of solid phosphorus are reported.

II. EXPERIMENTAL METHODS

The x-ray spectra were measured using a 12.7-cm, Johansson-type, curved-crystal spectrometer designed by Applied Research Laboratories.[12] This spectrometer is provided with a remotely controlled linear-wavelength drive which covers the Bragg angle range of 14.4°–71.8°. Other features of the spectrometer include fine adjustments for the crystal angle and focal circle radius. Modifications were made to the system so that these adjustments could be operated by remote control. A rotating crystal mount allows for the selection of one of two different crystals without having to disturb the spectrometer vacuum. In the present experiments, the detection element was a gas-flow proportional counter (operated with 90% argon and 10% methane) having a fixed entrance slit of 0.05-cm width. The counter operated at atmospheric pressure and was isolated from the vacuum by a 530 $\mu g/cm^2$ Mylar window. The Si and P measurements were performed with an EDDT (ethylene diamine ditartrate) crystal while all other spectra were obtained using an NaCl crystal.

A schematic diagram of the experimental configuration is shown in Fig. 1. The incident beam of 32.4-MeV O^{2+} ions was focused by means of two sets of quadrupole magnets and collimated to a diameter of 0.3 cm. A remotely driven target wheel was used to position the gas-target cell perpendicular to the incident ion beam. This target wheel, which could accommodate two gas-target cells along with a ZnS disk for viewing the beam, provided fine adjustment of the target position along the direction of the beam. The spectrometer was oriented in the horizontal plane so as to view x rays emitted at a mean angle of 142.5° with respect to the beam direction. The electronic system and method of data acquisition were the same as those described previously.[11]

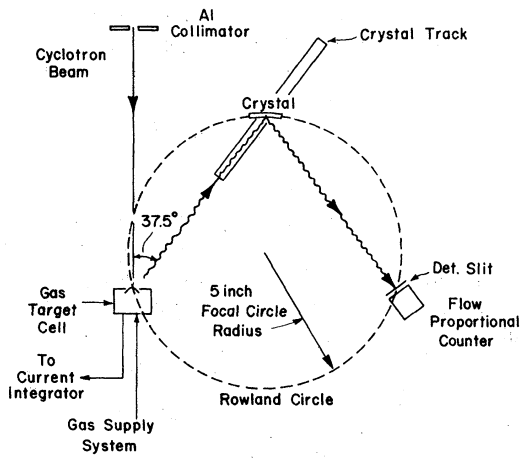

FIG. 1. Schematic diagram of the experimental arrangement.

The target gases were contained in small closed cells, each having a volume of 1.5 cm^3 and equipped with a 1.05-mg/cm^2 aluminized kapton window through which the beam entered and the x rays were viewed. The cells were operated at atmospheric pressure. Kapton ($C_{22}H_{10}N_2O_4$) was selected for the window material due to its strength, heat resistance, and x-ray-transmission efficiency. The calculated $K\alpha$ x-ray-transmission efficiencies through 1.32-mg/cm^2 kapton and 82-$\mu g/cm^2$ aluminum (corrected for observation angle) are 0.44, 0.69, 0.78, and 0.84 for Si, S, Cl, and Ar, respectively. The energy lost by the ion beam in passing through the gas-cell window was 8.9 MeV. It is assumed that the oxygen ions reached charge-state equilibrium in the gas-cell window and that they therefore entered the gas with an average charge of +6.5.[13]

In a typical run, one of the gas cells was mounted on the target wheel and attached to a gas manifold system by means of a piece of Tygon tubing. This arrangement enabled the evacuation and filling of the gas cell without disturbing its position and while the spectrometer system remained under vacuum. The other gas cell contained a solid reference target which was used for aligning and calibrating the spectrometer. Thick solid pellets of Si, S_8, and KCl were used to calibrate the spectrometer system for the measurements performed on Si, S, and Cl and Ar gases, respectively. Accurate energies for the $K\alpha$ satellites of these solids produced by 32-MeV oxygen-ion bombardment has previously been determined from calibrations carried out with 2.75-MeV protons.

It was found that a solid target could be moved several mm along the beam axis and x rays would still be detectable. Unfortunately, a displacement of the target also results in an apparent shift in the measured x-ray wavelength. This does not present a problem in the case of a solid, where the average depth for x-ray detection is on the order of 10^{-3} cm. Gases, however, are three orders of magnitude less dense and may have average depths for x-ray detection as great as

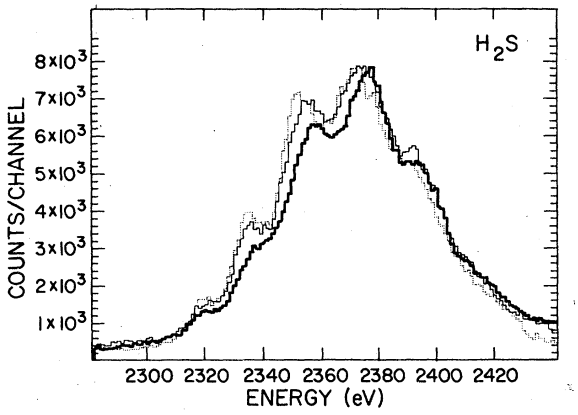

FIG. 2. Three time-sequenced spectra of H_2S showing the effect of decomposition: dark solid line, first spectrum; light solid line, second spectrum; dotted line, third spectrum.

0.5 cm. Hence a considerable amount of peak broadening is expected and observed in the present measurements with gases. Additional contributions to the peak widths will be discussed in Sec. IV.

Generally, at least three runs were made on each of the gases studied in which at least two spectra were measured consecutively to check the reproducibility. The light gases SiH_4, H_2S, and HCl tended to decompose with beam exposures of greater than 20 min at beam currents of 25 nA on target. An illustration of the effects of decomposition on the $K\alpha$ satellite spectrum of H_2S is shown in Fig. 2, where the heavy-line spectrum was succeeded by the light-line spectrum, which in turn was succeeded by the dotted-line spectrum. Decomposition was easy to recognize since consecutive spectra would show an intensification of

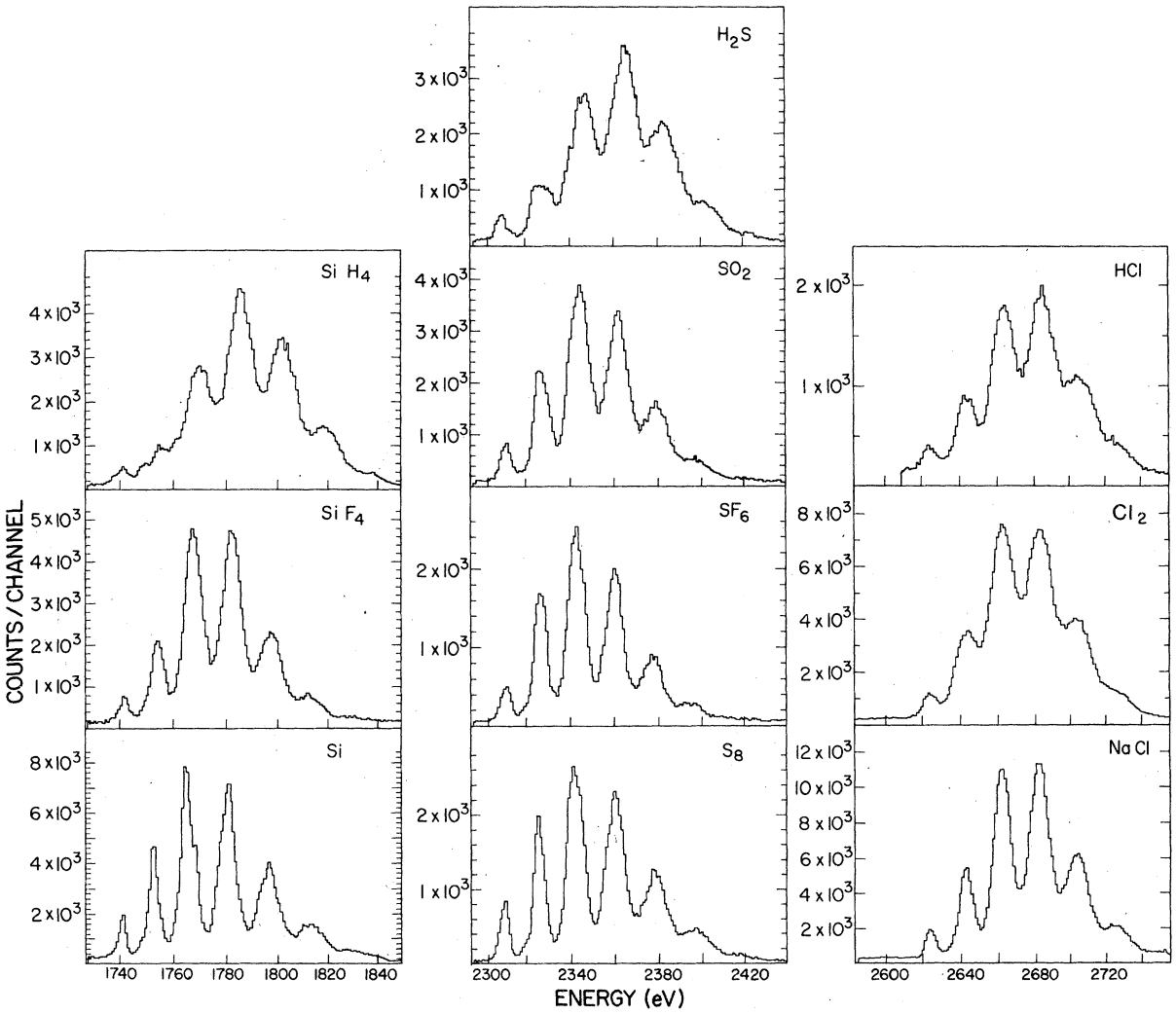

FIG. 3. A comparison of $K\alpha$ x-ray spectra for the various gaseous compounds of Si, S, and Cl studied with spectra for the corresponding reference solids.

the lower-order satellite peaks and a downward shift in their centroids. This effect resulted from the spectral overlap of the distribution of x rays arising from solid decomposition products that condensed on the inside surface of the gas-cell window with the distribution of x rays arising from the gas. In order to minimize this problem, the gas-cell window was replaced after every second spectrum.

III. ANALYSIS AND RESULTS

In Fig. 3, $K\alpha$ satellite spectra of the various gases of Si, S, and Cl studied in the present work are compared with the $K\alpha$ satellite spectrum of a solid target of the corresponding element. Aside from the increasing amount of peak broadening in going from the spectrum for the solid to the spectrum for the lightest gas (which is primarily due to the extensive path lengths for x-ray emission in the gases), the most noticeable feature in this comparison is the enhancement of the higher-order satellite intensities in the spectra for the light gases SiH_4, H_2S, and HCl over those displayed by the corresponding heavier gases and solids. The earlier work of Hopkins *et al.*[10] yielded this same observation. Further inspection of Fig. 3 shows that the spectra of the heavy gases SiF_4, SF_6, and Cl_2 are very similar to the spectra of the corresponding solids.

Shown in Fig. 4 is a comparison of the $K\alpha$ satellite spectra of liquid CCl_4 and solid NaCl. The

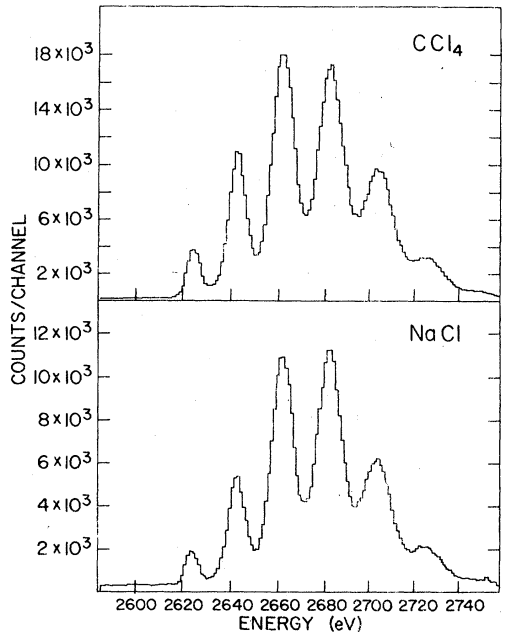

FIG. 4. A comparison of Cl $K\alpha$ x-ray spectra for liquid CCl_4 and solid NaCl.

CCl_4 spectrum is the first $K\alpha$ satellite spectrum reported for a compound in the liquid state and demonstrates the versatility of the closed-cell system used in the present experiments. It is apparent from the fact that the relative intensities of the second and third satellite peaks are more intense for CCl_4 than for NaCl that the apparent average state of L-shell ionization at the time of $K\alpha$ x-ray emission is lower for the liquid than for the solid.

All of the spectra were analyzed by means of a least-squares fitting program that employed a Gaussian-plus-exponential-tail fitting function. The resulting $K\alpha$ satellite peak intensities were then corrected for absorption in the target and for proportional counter detection efficiency using the procedures described in Ref. 11. In addition, a parameter p_L, which approximately represents the average fraction of L-shell electrons missing at the time of $K\alpha$ x-ray emission, was calculated for each spectrum by means of the formula

$$p_L = \frac{\bar{n}}{8} = \frac{1}{8}\sum_{n=1}^{7} n f_n , \tag{1}$$

where 8 is the number of L-shell electrons in the ground state and f_n is the corrected relative intensity of the nth satellite peak. This parameter concisely characterizes the overall satellite intensity distribution and is therefore quite useful for making detailed comparisons of the satellite distributions obtained for the various compounds. It should be noted, however, that p_L is of limited direct physical significance since an exact determination of the fraction of missing L-shell electrons must take into account the fact that the fluorescence yield is different for each satellite peak. Since the satellite intensity distribution depends on projectile energy, it was necessary to correct the p_L values to obtain values corresponding to the *incident* beam energy so that comparisons could be made with previous data obtained with solid compounds.[11] These corrections were accomplished by experimentally determining $\Delta p_L/\Delta E$ from spectra of solid targets taken with and without a kapton gas-cell window. The average beam energies for the detection of x rays were determined as in Ref. 11. Also, because the previous solid-target spectra were measured with a plane-crystal spectrometer, while the present spectra were measured with a curved-crystal spectrometer, small normalization corrections were required to account for differences in crystal reflectivities. These normalization corrections were determined experimentally by comparing solid-target spectra taken with both spectrometer systems, and they ranged from 1.03 for Si to 0.935 for Cl.

TABLE I. Relative intensities and p_L values for $K\alpha$ x-ray satellites produced by oxygen ions.

Compound	f_n $n=0$	$n=1$	$n=2$	$n=3$	$n=4$	$n=5$	$n=6$	$\bar{E}$ [a]	p_L [b]	$p_L^{(\mathrm{corr})}$ [c]	Γ_n
Silicon											
Si	0.032	0.113	0.259	0.275	0.192	0.090	0.038	18.4	0.363	0.330 ± 0.002	3.23
SiF_4	0.020	0.090	0.281	0.338	0.207	0.053	0.012	19.8	0.354	0.325 ± 0.002	2.69
SiH_4	0.011	0.055	0.170	0.318	0.295	0.121	0.029	18.1	0.414	0.387 ± 0.006	2.91
Phosphorus											
P_4	0.051	0.158	0.256	0.272	0.174	0.089		25.6	0.329	0.311 ± 0.002	3.10
Sulfur											
S_8	0.044	0.137	0.282	0.268	0.173	0.097		18.6	0.335	0.292 ± 0.002	3.05
SF_6	0.038	0.162	0.328	0.277	0.146	0.050		19.1	0.310	0.269 ± 0.006	2.78
SO_2	0.031	0.133	0.324	0.301	0.142	0.068		18.8	0.324	0.282 ± 0.010	2.77
H_2S	0.011	0.058	0.199	0.336	0.273	0.122		18.5	0.396	0.351 ± 0.006	2.63
Chlorine											
KCl	0.044	0.093	0.244	0.334	0.208	0.076		18.7	0.355	0.310 ± 0.003	2.86
NaCl	0.021	0.098	0.252	0.338	0.203	0.088		19.1	0.358	0.313 ± 0.003	2.75
CCl_4	0.029	0.123	0.255	0.311	0.192	0.090		18.5	0.348	0.303 ± 0.003	2.83
Cl_2	0.016	0.112	0.274	0.314	0.212	0.072		18.5	0.351	0.306 ± 0.008	2.79
HCl	0.023	0.090	0.210	0.366	0.227	0.084		18.4	0.367	0.321 ± 0.006	2.72
Argon											
Ar	0.013	0.093	0.267	0.396	0.171	0.060		18.7	0.350	0.309 ± 0.006	2.49
Potassium											
KCl	0.024	0.122	0.315	0.302	0.168	0.070		19.9	0.335	0.301 ± 0.005	2.74

[a] Calculated average beam energy (MeV) for the *detection* of $K\alpha$ x-rays. All measurements except those for P_4 were made with a kapton gas-cell window covering the target.
[b] p_L value determined directly from the corrected f_n.
[c] p_L value corrected for projectile energy loss and plane-crystal normalization.

Listed in Table I are the corrected $K\alpha$ satellite relative intensities for all of the targets investigated in the present work. Included in this table are the average beam energies for the detection of $K\alpha$ x rays and the p_L values before and after correction for projectile energy loss and plane-crystal spectrometer normalization. Another parameter of use in describing $K\alpha$ satellite intensity distributions is the distribution width Γ_n defined by the equation

$$\Gamma_n \simeq 2.35\sigma_n = 2.35\left(\sum f_n(n-\bar{n})^2\right)^{1/2}. \quad (2)$$

The distribution widths, which are also listed in Table I, are found to be consistently smaller for the gases than for the reference solids (except for NaCl). This difference increases markedly with Cl-ion projectiles.[10]

One final feature of interest in Fig. 3 is the relatively large energy shift displayed by a satellite in going from one compound of a given element to another. These energy shifts reflect the effect of M-shell vacancies on the $K\alpha$ satellite energies and together with Hartree-Fock calculations provide a measure of the effective number of M-shell electrons missing at the time of $K\alpha$ x-ray emission. Listed in Table II are $K\alpha$ satellite peak centroid energies for all of the targets investigated in the present work. Also given in this table are the average energies of the $K\alpha$ satellite distributions $\bar{E}_x$ calculated according to the equation

$$\bar{E}_x = \sum_{n=0}^{7} f_n E_{KL}n. \quad (3)$$

IV. DISCUSSION

A. Satellite relative intensities

The present results for the heavy gases and the liquid follow essentially the same trends as those observed previously for solids.[11] Shown in Fig. 5 is a comparison of the p_L values for solid and gaseous compounds of Si, S, and Cl, and the liquid CCl_4 plotted as a function of effective charge. The effective charge of an atom in a compound is a measure of its local valence-electron density and is here calculated from the product of the oxidation number and the Pauling bond ionicity.[14] In each of the chemical series it is seen that p_L decreases smoothly with increasing effective charge. While

TABLE II. Energies (in eV) of $K\alpha$ satellite peaks produced by oxygen ions.

Compound	KL^0	KL^1	KL^2	KL^3	KL^4	KL^5	KL^6	$\bar{E}_x$
Silicon								
Si	1739.8±0.1	1751.2±0.5	1763.9±0.3	1778.7±0.6	1794.0±0.3	1809.3±0.5	1826.8±0.7	1776.3
SiF_4	1740.6±0.6	1752.8±0.5	1766.0±0.3	1780.4±0.6	1795.3±0.3	1809.6±0.5	1826.0±0.7	1780.0
SiH_4	1739.6±0.6	1754.3±1.0	1768.0±0.7	1783.6±0.8	1799.4±0.8	1815.4±0.7	1831.2±0.7	1787.0
Phosphorus								
P_4	2013.4±0.3	2026.0±0.3	2040.2±0.3	2056.7±0.3	2074.2±0.4	2092.1±0.4		2051.6
Sulfur								
S_8	2308.6±0.5	2323.7±0.4	2339.8±0.2	2357.9±0.5	2376.2±0.7	2395.4±0.7		2355.1
SF_6	2309.3±0.5	2324.8±0.4	2340.7±0.4	2357.9±0.5	2375.3±0.7	2393.4±0.7		2351.7
SO_2	2309.4±0.5	2325.0±0.7	2341.9±0.4	2359.4±0.5	2377.0±0.7	2394.2±0.7		2350.1
H_2S	2308.7±0.9	2325.8±0.6	2343.7±0.3	2361.8±0.7	2380.0±0.7	2398.5±0.7		2362.6
Chlorine								
KCl	2621.4±0.5	2640.4±0.5	2659.0±0.4	2679.1±0.4	2699.0±0.7	2719.9±0.7		2672.6
NaCl	2621.7±0.5	2640.2±0.4	2659.0±0.5	2678.8±0.4	2698.9±0.7	2720.2±0.8		2676.6
CCl_4	2622.3±0.5	2640.1±0.4	2658.8±0.5	2679.0±0.4	2699.0±0.7	2719.9±0.8		2674.9
Cl_2	2621.5±0.8	2640.7±0.7	2660.1±0.7	2680.5±0.6	2700.7±0.7	2721.7±0.8		2676.8
HCl	2619.2±0.7	2640.1±1.6	2659.3±1.9	2680.3±1.8	2701.0±1.2	2721.7±1.5		2679.1
Argon								
Ar	2957.0±0.9	2975.8±1.1	2996.5±0.8	3018.3±0.8	3041.2±0.8	3061.9±0.9		3014.3
Potassium								
KCl	3314.1±1.0	3335.1±0.9	3356.4±1.0	3378.7±1.1	3402.4±1.1	3428.1±0.9		3375.6

the p_L values for the gases SO_2, SF_6, Cl_2, and the liquid CCl_4 are consistent with the trend established by the solid compounds, it is apparent that the p_L values for the gases SiH_4, H_2S, and HCl lie well above the smooth line drawn through the other data points.

Another measure of the local valence-electron density of an atom in a compound is provided by inner-shell-electron binding-energy shifts as measured by electron spectroscopy for chemical analysis (ESCA). Shown in Fig. 6 is a comparison of p_L with measured $2p$-electron binding-energy shift for those compounds for which binding energy shifts are available from the literature (sulfur and silicon compounds and CCl_4 from Ref. 15, chlorine solids from Ref. 16, and HCl from Ref. 17). In evaluating the binding-energy shifts of the gases relative to the binding energy of the reference solid, it was necessary to correct for the work function of the solid since binding energies of solids are usually measured relative to the Fermi level. The work function was taken to be 4.5 eV for Si and 4.6 eV for S and Cl.[18]

Examination of Fig. 6 reveals essentially the same features as displayed by the correlations with effective charge. Since the heavy gases and the liquid have p_L values that closely fit the trend established by the data for solids, it is concluded that the rearrangement processes, in general, do not depend upon physical state. The question of whether or not rearrangement depends on physical state really relates to the relaxation time of the system relative to the lifetime of a K-shell vacancy. In a gas, electrons can only be transferred from the atoms which comprise the individual molecule, whereas in a solid, electrons can, in principle, by supplied by a large number of atoms in the surrounding region of the crystal lattice. The present results indicate that it is primarily electron transfer from nearest-neighbor atoms

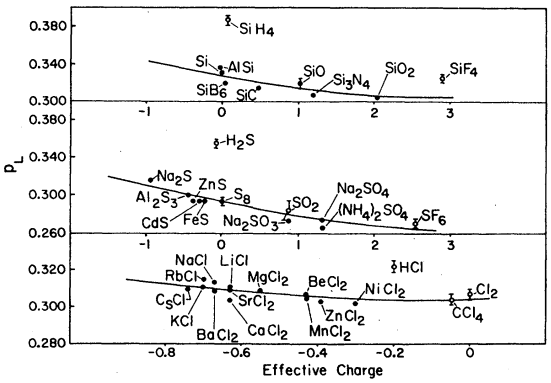

FIG. 5. The variation of p_L with effective charge for compounds of Si, S, and Cl excited by oxygen ions. The solid data points are from Ref. 11 and the open data points are from the present measurements for gases.

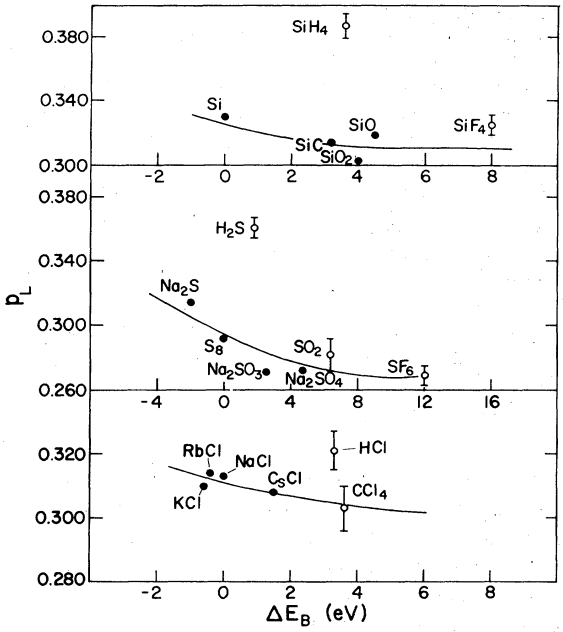

FIG. 6. The variation of p_L with $2p$-electron binding-energy shift as measured by ESCA (Refs. 15–17). The solid data points are from Ref. 11 and the open data points are from the present measurements for gases.

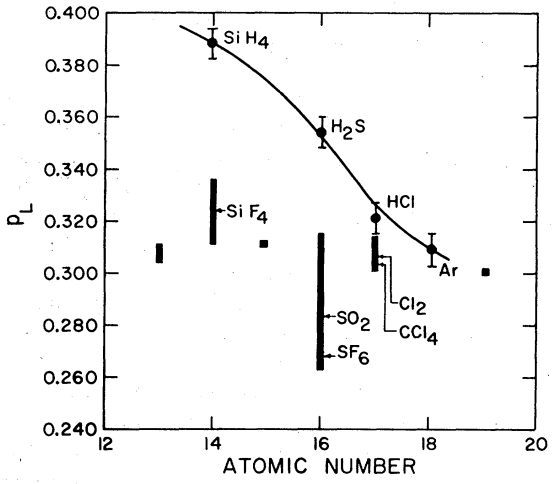

FIG. 7. The variation of p_L with target atomic number. The p_L values for the light gases (SiH_4, H_2S, HCl, and Ar) are indicated by the data points through which a smooth curve has been drawn. The *ranges* of the p_L values for solid compounds are shown by the solid bars and the locations of the p_L values for the heavy gases (SiF_4, SO_2, SF_6, Cl_2) and the liquid (CCl_4) are indicated by arrows.

that gives rise to the observed effects on $K\alpha$ x-ray satellites.

The behavior of p_L as a function of effective charge and binding energy shift can be understood by considering the availability of valence electrons immediately following the collision. In those atoms having low effective charges and binding-energy shifts, the valence electrons of the compound are mainly localized in the vicinity of the target atom before the collision and are therefore mostly ionized during the collision. This depletion of the total valence-electron population results in a high p_L value. At more positive values of the effective charge and binding-energy shift, the valence electrons spend less time in the vicinity of the target atom and more time displaced toward neighboring atoms, in which case they are not as likely to be ionized in the collision. Following the collision, these valence electrons are readily available to participate in K-, L-, and M-vacancy filling transitions thereby leading to lower p_L values. The descrease in p_L with increasing effective charge appears to level off at high positive values. This indicates that a saturation point is reached beyond which an increase in the available number of valence electrons has no significant effect on the rates of rearrangement transitions.

The dependence of p_L on target atomic number is shown in Fig. 7. In this figure, the p_L values for the light gases are indicated by the data points through which a smooth curve has been drawn. The *ranges* of the p_L values for solid compounds are shown by the solid bars, and the locations of the p_L values for the heavy gases and the liquid are indicated by arrows. Examination of Fig. 7 reveals the following:

(a) The gases SiH_4, H_2S, and HCl are again seen to have much larger p_L values than do the corresponding gases having ligands containing large numbers of valence electrons (i.e., SiF_4, SO_2, SF_6, and Cl_2). In addition, the p_L values for the hydrated gases decrease monotonically with increasing target atomic number and converge with the solid compound values near $Z = 18$.

(b) The gases SiF_4, SO_2, SF_6, and Cl_2 and the liquid CCl_4 have p_L values which fall within the ranges observed for the corresponding solids.

The extraordinarily high p_L values displayed by the gases SiH_4, H_2S, and HCl result from the fact that following a collision the Si, S, and Cl atoms exist in essentially a free-atom environment in which only intra-atomic $M \rightarrow K$ and $M \rightarrow L$ electron transitions can contribute to a lowering of p_L. It is apparent from the rapid decrease in p_L in going from SiH_4 to H_2S to HCl to Ar that the importance of intra-atomic rearrangement greatly increases as the population of the $3p$ level increases. The large difference in p_L between SiH_4 and the other Si compounds directly reflects the importance of interatomic rearrangement processes in atoms having highly depleted M shells. A more quantitative discussion of M-shell popula-

tions at the time of $K\alpha$ x-ray emission will be given in the following section.

B. Satellite energies

Comparison of the experimental $K\alpha$ satellite energies with the results of accurate energy calculations enables the determination of the effective degree of M-shell ionization present at the time of x-ray emission. In the present work, the Hartree-Fock program of Fischer[19] was used to calculate the total energies for the initial and final states associated with each KL^nM^m vacancy configuration of Si and S atoms. For all cases, the option of calculating an average of configurations was utilized so that a single energy was calculated for the KL^0 and KL^7 peaks, two energies were calculated for the KL^1 and KL^6 peaks and three energies were calculated for peaks KL^2 through KL^5. For example, in the case of a KL^1 peak, the average energy for the two initial states (^1S, ^3S) arising from the vacancy configuration $1s^{-1}2s^{-1}$ and the average energy for the two initial states (^1P, ^3P) arising from the vacancy configuration $1s^{-1}2p^{-1}$ were calculated. The $1s^{-1}2s^{-1}$ states may decay by $K\alpha$ x-ray emission to ^1P and ^3P final states for which an average energy was calculated and the $1s^{-1}2p^{-1}$ may decay to ^1S or ^1D, and ^3P final states for which an average energy was calculated. Thus for each state of M-shell ionization the energies of 21 initial states and 21 final states were calculated. The x-ray satellite transition energies were then obtained by taking the differences in total energies for the initial and final states.

The energies calculated by the Fischer Hartree-Fock program are not exact for two reasons: (a) the calculation is nonrelativistic, and (b) the Hartree-Fock method does not fully account for electron correlation. However, for the low-Z atoms of interest here, the correlation energy correction is expected to be less than one eV.[20] The relativistic energy correction may be estimated by comparing experimental and calculated transition energies for well defined configurations. The calculated normal $K\alpha$ transition energy for Si (1737 eV) and S (2302 eV) are, respectively, 3 eV and 5 eV lower than the experimental energies given by Bearden.[21] A determination of the magnitudes of the energy corrections required for multiple-vacancy configurations of sulfur is possible using the measurements of Panke *et al.*[22] These investigators have reported $K\alpha$ satellite and hypersatellite transition energies for 92-MeV sulfur projectiles which are thought to be fully stripped beyond the L shell. The experimental energies are compared with the results of the Hartree-Fock calculations in Table III. It was assumed that the satellite transition energy correction varies linearly with the number of L-shell vacancies, and based on the differences between the calculated and experimental KL^0 transition energies and the results of the comparisons given in Table III, corrections ranging from 3 and 5 eV for the KL^0 energies to 5 and 9 eV for the KL^7 energies of Si and S, respectively, were added to the calculated satellite transition energies.

TABLE III. Comparison of experimental and calculated $K\alpha$ satellite and hypersatellite energies (in eV) for sulfur atoms having fully stripped M shells.

Peak	E_{exp} [a]	E_{HF}	$E_{exp}-E_{HF}$
KL^6	2428.2 [b]	2420.6 [c]	7.6
KL^7	2454.7 [b]	2442.9	11.8
K^2L^6	2596.2	2587.7	8.5
K^2L^7	2621.6	2612.2	9.4

[a] From Ref. 22.
[b] Weighted average energy of all transitions contributing to the designated peak.
[c] Statistical average of $1s^{-1}2s^{-2}2p^{-4} \rightarrow 2s^{-2}2p^{-5}$ and $1s^{-1}2s^{-1}2p^{-5} \rightarrow 2s^{-1}2p^{-6}$ transition energies.

The calculated energy differences ($E_{KL^n}-E_{KL^0}$) for Si and S $K\alpha$ x rays are plotted in Fig. 8 as a function of the number of M-shell vacancies. Also shown in this figure are the measured energy differences for Si, SiF_4, and SiH_4, and for S_8, SF_6, and H_2S. The intersection points of the measured energy differences with the calculated energy differences have been connected by straight lines to more clearly delineate the variation of the estimated number of M-shell vacancies from satellite to satellite and to facilitate a comparison of the patterns displayed by the different compounds. It is immediately apparent that the numbers of M-shell vacancies present for the light gases SiH_4 and H_2S are significantly larger than for the corresponding heavy gases and solids.

A similar analysis was carried out for argon using the results of Hartree-Fock-Slater (HFS) transition-energy calculations reported by Bhalla.[23] Although HFS energies are generally not as accurate as Hartree-Fock energies due to the limitations of the exchange approximation, it has been found that the values of ($E_{KL^n}-E_{KL^0}$) calculated by both methods agree to within 2 eV for the $K\alpha$ satellites of Al, Cl, and K.[24,25] Therefore the HFS results reported in Ref. 23 are considered accurate enough to provide a comparative estimate of the number of M-shell vacancies associated with each satellite line of argon. (Energy corrections scaled from those used for S were added to the HFS satellite energies.) Using these estimates and the estimates provided by Fig. 8, the average number of M-shell vacancies $\bar{m}$ were cal-

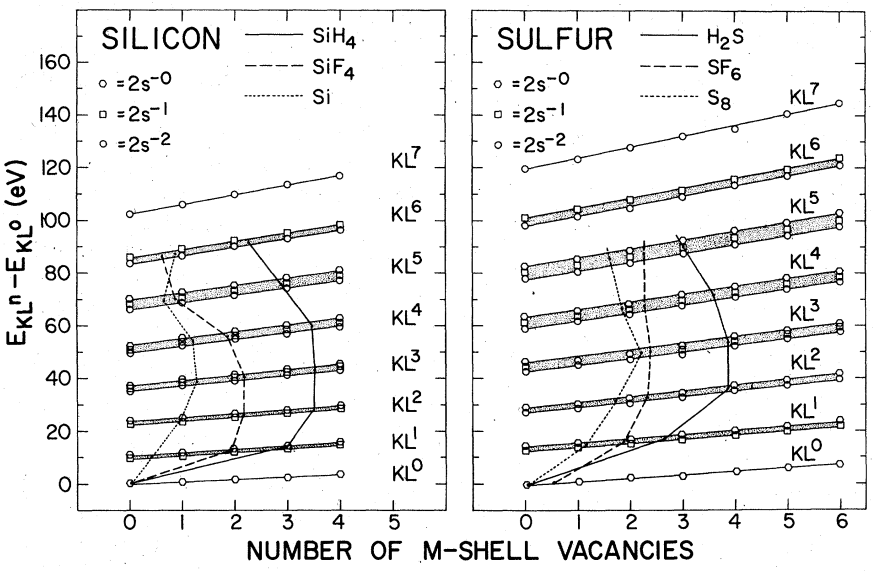

FIG. 8. Calculated (Hartree-Fock) $K\alpha$ satellite energy differences (measured relative to the KL^0 energy) plotted as a function of the number of M-shell vacancies. The intersection points of the measured energy differences for several compounds with the calculated curves are connected by straight line segments.

culated for the various compounds considered according to the formula

$$\bar{m} = \sum_{n=0}^{7} m_n f_n . \tag{4}$$

The average numbers of M-shell vacancies obtained from this analysis are listed in Table IV.

It is evident from Table IV that the solids Si and S_8 are missing about 25% of their M-shell electrons at the time of $K\alpha$ x-ray emission, while the gases SiH_4 and H_2S are missing approximately 83% and 60% of their M-shell electrons, respectively. This observation is consistent with the fact that in SiH_4 and H_2S there are very few valence electrons available to replace those which are ionized in the collision.[10] In the cases of solid Si and S_8, however, valence electrons are readily available from neighboring atoms and are apparently transferred to the struck atom prior to $K\alpha$ x-ray emission. (A valence electron having a binding energy of 6 eV has an average velocity sufficient to travel 150 Å in 10^{-14} sec.) The lower states of M-shell ionization exhibited by the heavy gases and solids over those exhibited by the light gases indicate that interatomic electron transfer to the M shell together with intra-atomic $M \rightarrow L$ and $M \rightarrow K$ transitions may account for a substantial part of the observed changes in the p_L values for these compounds. However, it is interesting to note that in spite of the fact that SiF_4 and SF_6 have more M-shell vacancies than Si and S_8, they nevertheless have *lower* p_L values. This may be interpreted as evidence that rearrangement does not occur solely by $M \rightarrow M$ electron transfer with subsequent intra-atomic $M \rightarrow L$ and $M \rightarrow K$ decay, but must also involve direct interatomic $M \rightarrow L$ transfer.

C. Satellite peak widths

As mentioned in Sec. II, a large portion of the satellite peak width observed for the gaseous compounds is attributable to instrumental broadening associated with the extensive path length for x-ray emission from the target. Other peak-broadening mechanisms exist which, in principle, can also contribute to the total peak width.

1. Molecular dissociation

In a highly ionizing collision between a heavy ion and a gas molecule, it is to be expected that the gas molecule will undergo dissociation. If an x ray is emitted as the two charged molecular fragments accelerate away from each other as a result of Coulomb repulsion, it will experience a Doppler shift. Such a kinematic broadening effect has indeed been observed for K-Auger transitions in carbon and nitrogen containing molecules under bombardment by 56-MeV Ar ions.[26] The line-broadening component of the 318-eV KL_1L_2 Auger line associated with the molecular dissociation of N_2 was found to be 6.85 eV.

TABLE IV. Estimated average number of missing M-shell electrons and average M-vacancy fractions.

Compound	$\bar{m}$	p_M
Si	1.0	0.25
SiF_4	2.0	0.50
SiH_4	3.3	0.83
S_8	1.7	0.28
SF_6	2.2	0.37
H_2S	3.6	0.60
Ar	2.9	0.36

A straightforward application of the laws of conservation of momentum and energy yields the following expression for the velocity of a molecular fragment v_1 having mass m_1 and charge q_1e:

$$v_1 = \left[\frac{2q_1q_2e^2}{R}\,\frac{m_2}{m_1(m_1+m_2)}\right]^{1/2}, \tag{5}$$

where R is the equilibrium-bond distance between the two fragments and m_2 and q_2e are the mass and charge, respectively, of the other fragment. An x ray emitted from fragment 1 will be Doppler shifted by an amount

$$\Delta E \simeq E_0\beta_1\cos\theta, \tag{6}$$

where $\beta_1 = v_1/c \ll 1$, E_0 is the emitted x-ray energy, and θ is the angle of emission relative to the velocity vector of the fragment. Consider, as an example, the molecular dissociation of H_2S into H and HS. The estimated most probable charge state of the HS fragment is 8+, corresponding to one K-, three L-, and four M-shell vacancies. If the H fragment is assumed to have a charge of 1+, the maximum Doppler broadening ($\sim 2E_0\beta_1$) amounts to 0.06 eV for a sulfur $K\alpha$ x ray. A similar calculation for the breakup of Cl_2 into Cl^{6+} and Cl^{3+} yields a maximum Doppler broadening of 0.33 eV. The actual Doppler broadening will be less than the above estimates for two reasons: (a) the fragments are distributed more or less isotropically so that θ will not always be 0° or 180°, and (b) the lifetime of the $K\alpha$ x ray is so short that only metastable transitions will be Doppler broadened by the full dissociation velocity.[26] It is therefore concluded that molecular dissociation does not cause a significant amount of broadening in the present experiments.

2. Recoil

Doppler broadening is also a consequence of the transfer of recoil momentum to the target atom by the projectile during the collision. The amount of energy Q that the target atom gains through recoil is given by[27]

$$Q = \frac{2}{M_2}\left(\frac{Z_1Z_2e^2}{V}\right)^2\frac{1}{X^2+(b/2)^2}, \tag{7}$$

where M_2 and Z_2^e are the mass and nuclear charge of the target atom, Z_1e is the nuclear charge of the projectile, V is the velocity of the projectile (in the laboratory system of coordinates), X is the impact parameter, and b is the distance of closest approach given by

$$b = Z_1Z_2e^2/E_{\text{c.m.}} \tag{8}$$

in which $E_{\text{c.m.}}$ is the center of mass energy. Consider as an example of this type of broadening the case of a 23.5-MeV oxygen ion incident on a free sulfur atom. Taking the radius of maximum K-electron density, 3.35×10^{-10} cm,[28] as the most probable impact parameter for K-shell ionization results in a calculated recoil energy of 64 eV. This corresponds to a target atom (laboratory) recoil angle of 89.9° with respect to the incident beam direction. Applying Eq. (6) to calculate the Doppler shift of a sulfur $K\alpha$ x ray emitted at the maximum and minimum emission angles relative to the spectrometer, $\theta_1 = 127.6°$ and $\theta_2 = 52.6°$, leads to an estimated broadening of $\Delta E = 0.19$ eV. It is therefore concluded that target-atom recoil does not cause a significant amount of broadening in the present experiments.

3. M-shell vacancy distribution

The results of the Hartree-Fock calculations presented in Sec. IV B can be used to show how the distribution of M-shell vacancies leads to a significant spread in energy for each KL^n transition depending upon the number of M-shell electrons present at the time of $K\alpha$ x-ray emission. In sulfur, a particular KL^n peak can vary in energy from 7 eV for the KL^0 peak up to 25 eV for the KL^7 peak according to the M-shell configuration.

Since the distribution of M-shell vacancies for each KL^n transition was not determined experimentally, it will be assumed that the distribution of M-shell vacancies is binomial in character, as is the distribution of L-shell vacancies.[24,29] Then the relative probability of producing a particular M-shell configuration, P_M, can be calculated from

$$P_M = \binom{N_M}{m} p_M^m(1-p_M)^{N_M-m}, \tag{9}$$

where $\binom{N_M}{m}$ is the binomial coefficient, m is the number of M-shell vacancies, and p_M is as given in Table IV.

The full width at half maximum (FWHM) Γ_M of the M-shell vacancy distribution is approximately given by

$$\Gamma_M \simeq 2.35\left(\sum_m P_M(m-\bar{m})^2\right)^{1/2}. \tag{10}$$

Thus Γ_M can be used to determine ΔE_M, the energy broadening due to the spread in M-shell vacancies, from the Hartree-Fock calculated energy values for each $K\alpha$ satellite peak.

At this point, it is of interest to see if a full account of the total peak widths observed for the gaseous compounds may be accomplished. The total width of a KL^n peak, ΔE_T, can be approximated by four width components:

$$\Delta E_T = (\Delta E_{sp}^2 + \Delta E_p^2 + \Delta E_M^2 + \Delta E_{\text{Mult}}{}^2)^{1/2}, \tag{11}$$

TABLE V. $K\alpha$ satellite peak width components (all energies in eV).

Compound	ΔE_{sp}	ΔE_p	ΔE_M	ΔE_{mult}	$\Delta E_{T(calc)}$	$\Delta E_{T(exp)}$
SiH_4	3.7	7.0	3.0	4.1	9.4	9.8±0.6
H_2S	5.6	5.3	7.3	6.1	12.2	13.5±0.6
HCl	6.0	10.5	8.8	7.0	16.5	16.8±1.0
Ar	9.1	16.1	9.7	8.0	22.4	21.3±1.0

where ΔE_{sp} is the resolution of the spectrometer (FWHM), ΔE_p is the predicted broadening for gases due to path length, ΔE_M is the broadening due to the distribution of M-shell vacancies, and ΔE_{Mult} is a width factor associated with the fact that each peak is composed of overlapping multiplet lines. The resolution of the spectrometer was determined from the FWHM of the KL^0 peak of the reference solid. The predicted path-length broadening for the gases ΔE_p was determined from calculated effective path lengths and peak energy shifts measured with the reference solids as a function of target position. The multiplet width factor ΔE_{Mult} was taken to be the residual width of the reference solid peak after the ΔE_{sp} and ΔE_M width components had been removed. Table V lists the results obtained by applying the above analysis to the third satellite peak of several of the gases investigated. The third satellite peak was chosen for comparison since it was generally the most intense peak. It is concluded on the basis of the good agreement between the calculated and observed total widths listed in Table V that the peak widths are consistent with expectations based upon consideration of the various possible broadening mechanisms, and that the widths observed for the gases, after correction for path-length effects and M-shell vacancy broadening, are the same as those observed for solids.

V. CONCLUSION

In the present investigation, the $K\alpha$ satellite spectra of gaseous compounds of silicon, sulfur, and chlorine, liquid CCl_4, and gaseous Ar, produced by 32.4-MeV oxygen ions, have been compared to those obtained in a previous study of solid compounds of elements within the same range of atomic number to demonstrate the relative contribution of interatomic vacancy transfer to electron rearrangement occurring on a time scale of 10^{-14} sec. It was found that the apparent degree of L-shell ionization for the compounds studied did not depend upon the physical state but rather upon the availability of electrons from nearest-neighbor atoms.

A comparison of the experimentally measured $K\alpha$ satellite energy shifts with the results of Hartree-Fock calculations demonstrated that electron transfer to the M shell is highly probable in systems having available valence electrons on neighboring atoms. What has yet to be determined is the extent to which L- and K-vacancy transfer are accomplished directly by interatomic $M \rightarrow L$ and $M \rightarrow K$ transitions versus interatomic $M \rightarrow M$ transitions with a subsequent intra-atomic cascade of $M \rightarrow L$ and $M \rightarrow K$ transitions. Evidence for direct interatomic electron transfer to all three levels is provided by the fact that Si and S_8 have higher p_L values than do SiF_4 and SF_6, even though the satellite energy shifts show that SiF_4 and SF_6 have more M-shell vacancies than do Si and S_8.

A determination of the various components of the peak widths, including spectrometer resolution, path-length broadening in low-density gases, M-shell vacancy broadening, and a residual factor due to multiplet structure, was shown to be in good agreement with the experimentally observed peak widths. Other sources of broadening, such as Doppler shift arising from molecular dissociation and target-atom recoil, were shown to be insignificant in this work.

ACKNOWLEDGMENTS

We wish to thank John White, Alice Leeper, Mark Michael, and Jeffrey Sjurseth for their help with the experiments and assistance with the data processing. The support of the cyclotron staff is gratefully acknowledged with special credit going to Wilmer Walterscheid, Walter Chapman, and Molly Allen. This work was supported by the Robert A. Welch Foundation and the Air Force Institute of Technology.

*Present address: Air Force Weapons Laboratory, Kirtland Air Force Base, Albuquerque, N.M. 87117.

[1]V. F. Demekhin and V. P. Sachenko, Bull. Acad. Sci. USSR 31, 921 (1967).
[2]K. Laüger, J. Phys. Chem. Solids 33, k343 (1972).
[3]P. Richard, J. Bolger, D. K. Olsen, and C. F. Moore, Phys. Lett. 41A, 269 (1972).
[4]P. G. Burkhalter, A. R. Knudson, D. J. Nagel, and K. L. Dunning, Phys. Rev. A 6, 2093 (1972).
[5]J. McWherter, D. K. Olsen, H. H. Wolter, and C. F. Moore, Phys. Rev. A 10, 200 (1974).
[6]R. L. Watson, T. Chiao, and F. E. Jenson, Phys. Rev. Lett. 35, 254 (1975).
[7]C. F. Moore, D. L. Matthews, and H. H. Wolter, Phys. Lett. 54A, 407 (1975).
[8]R. L. Kauffman, K. A. Jamison, T. J. Gray, and P. Richard, Phys. Rev. Lett. 36, 1074 (1976).
[9]F. Hopkins, J. Sokolov, and A. Little, Phys. Rev. A 14, 1907 (1976).
[10]F. Hopkins, A. Little, N. Cue, and V. Dutkiewicz, Phys. Rev. Lett. 37, 1100 (1976).
[11]R. L. Watson, A. K. Leeper, B. I. Sonobe, T. Chiao, and F. E. Jenson, Phys. Rev. A 15, 914 (1977).
[12]Applied Research Laboratories, P. O. Box 129, Sunland, Calif. 91040, Catalog No. 132675.
[13]A. B. Wittkower and H. D. Betz, At. Data 5, 113 (1973).
[14]L. Pauling, *The Nature of the Chemical Bond* (Cornell University, Ithaca, N.Y., 1960).
[15]T. A. Carlson, *Photoelectron and Auger Spectroscopy* (Plenum, New York, 1975).
[16]C. K. Jorgensen and H. Berthou, K. Dan. Vidensk. Selsk. Mat.-Fys. Medd. 38, No. 1 (1972).
[17]D. B. Adams, J. Electron Spectrosc. Relat. Phenom. 10, 247 (1977).
[18]*Handbook of Chemistry and Physics*, edited by R. C. Weast (Chemical Rubber, Cleveland, Ohio, 1976).
[19]C. F. Fischer, Comput. Phys. Commun. 1, 151 (1969).
[20]T. Åberg, Phys. Rev. 162, 5 (1967).
[21]J. A. Bearden, Rev. Mod. Phys. 39, 88 (1967).
[22]H. Panke, F. Bell, H. D. Betz, and W. Stehling, Nucl. Instrum. Methods 132, 25 (1976).
[23]C. P. Bhalla, Phys. Rev. A 8, 2877 (1973).
[24]R. L. Watson, F. E. Jenson, and T. Chiao, Phys. Rev. A 10, 1230 (1974).
[25]P. Richard, Phys. Fenn. 9, 3 (1974); Proceedings of the International Conference on X-ray Processes in Matter, Otaniemi, Finland, 28 July–1 August 1974 (unpublished).
[26]R. Mann, Folkmann, and K.-O. Groeneveld, Phys. Rev. Lett. 37, 1674 (1976).
[27]R. D. Evans, *The Atomic Nucleus* (McGraw-Hill, New York, 1972), p. 847.
[28]J. P. Desclaux, At. Data Nucl. Data Tables 12, 311 (1973).
[29]R. L. Kauffman, J. H. McGuire, P. Richard, and C. F. Moore, Phys. Rev. A 8, 1233 (1973).